DOI: 10.1021/ic101064c

Inorganic Chemistry
Article

Heterospin π-Heterocyclic Radical-Anion Salt: Synthesis, Structure, and Magnetic Properties of Decamethylchromocenium [1,2,5]Thiadiazolo[3,4-*c*][1,2,5]thiadiazolidyl

Nikolay A. Semenov,[†] Nikolay A. Pushkarevsky,[‡] Anton V. Lonchakov,[§,∥] Artem S. Bogomyakov,[⊥] Elena A. Pritchina,[§,¶] Elizaveta A. Suturina,[§,∥] Nina P. Gritsan,*[,§,∥] Sergey N. Konchenko,[‡] Ruediger Mews,[□] Victor I. Ovcharenko,[⊥] and Andrey V. Zibarev*[,†,∥]

[†]*Institute of Organic Chemistry,* [‡]*Institute of Inorganic Chemistry,* [§]*Institute of Chemical Kinetics & Combustion, and* [⊥]*International Tomography Center, Siberian Branch of the Russian Academy of Sciences, Novosibirsk, Russia,* [∥]*Department of Physics,* [¶]*Department of Natural Sciences, Novosibirsk State University, Novosibirsk, Russia, and* [□]*Institute for Inorganic and Physical Chemistry, University of Bremen, Bremen, Germany*

Received May 26, 2010

Decamethylchromocene, $Cr^{II}(\eta^5\text{-}C_5(CH_3)_5)_2$ (**2**), readily reduced [1,2,5]thiadiazolo[3,4-*c*][1,2,5]thiadiazole (**1**) in a tetrahydrofuran solvent at ambient temperature with the formation of radical-anion salt $[\mathbf{2}]^+[\mathbf{1}]^-$ (**3**) isolated in 97% yield. The heterospin salt **3** ($[\mathbf{2}]^+$, $S = {}^3/_2$; $[\mathbf{1}]^-$, $S = {}^1/_2$) was characterized by single-crystal X-ray diffraction as well as magnetic susceptibility measurements in the temperature range 2−300 K. The experimental data together with theoretical analysis of the salt's magnetic structure within the CASSCF and spin-unrestricted broken-symmetry (BS) density functional theory (DFT) approaches revealed antiferromagnetic (AF) interactions in the crystalline **3**: significant between anions $[\mathbf{1}]^-$, weak between cations $[\mathbf{2}]^+$, and very weak between $[\mathbf{1}]^-$ and $[\mathbf{2}]^+$. Experimental temperature dependences of the magnetic susceptibility and the effective magnetic moment of **3** were very well reproduced in the assumption of the AF-coupled $[\mathbf{1}]^-\cdots[\mathbf{1}]^-$ ($J_1 = -40 \pm 9$ cm^{-1}) and $[\mathbf{2}]^+\cdots[\mathbf{2}]^+$ ($J_2 = -0.58 \pm 0.03$ cm^{-1}) pairs. The experimental J_1 value is in reasonable agreement with the value calculated using BS UB3LYP/6-31+G(d) (−61 cm^{-1}) and CASSCF(10,10)/6-31+G(d) (−15.3 cm^{-1}) approaches. The experimental J_2 value is also in agreement with that calculated using the BS DFT approach (−0.33 cm^{-1}).

Introduction

Chalcogen−nitrogen open-shell π-heterocyclic systems, both neutral and charged, are of interest to fundamental chemistry and its applications in the field of functional materials.[1−4] During the past 2 decades, numerous chalcogen−nitrogen π-heterocyclic neutral radicals and radical cations were synthesized and successfully used as building blocks in the design and synthesis of both molecular magnets and conductors,[2−4] whereas radical anions (RAs; known since the 1960s from electron spin resonance experiments)[5] remained a missing link because of the lack of approaches to their isolation.

Recently, it was found that some derivatives of the 1,2,5-chalcogenadiazole ring system (chalcogen: S, Se), in particular

*To whom correspondence should be addressed. E-mail: gritsan@kinetics.nsc.ru (N.P.G.), zibarev@nioch.nsc.ru (A.V.Z.).

(1) (a) Chivers, T.; Laitinen, R. S. In *Handbook of Chalcogen Chemistry. New Perspectives in Sulfur, Selenium and Tellurium*; Devillanova, F., Ed.; RSC Press: Cambridge, U.K., 2007. (b) Chivers, T. *A Guide to Chalcogen-Nitrogen Chemistry*; World Scientific: Singapore, 2005.

(2) (a) Mito, M.; Komorida, Y.; Tsuruda, H.; Tse, J. S.; Desgreniers, S.; Ohishi, Y.; Leitch, A. A.; Cvrkalj, K.; Robertson, C. M.; Oakley, R. T. *J. Am. Chem. Soc.* **2009**, *131*, 16012–16013. (b) Robertson, C. M.; Leitch, A. A.; Cvrkalj, K.; Reed, R. W.; Myles, D. J. T.; Dube, P. A.; Oakley, R. T. *J. Am. Chem. Soc.* **2008**, *130*, 8414–8425. (c) Robertson, C. M.; Myles, D. J. T.; Leitch, A. A.; Reed, R. W.; Dooley, B. M.; Frank, N. L.; Dube, P. A.; Thompson, L. K.; Oakley, R. T. *J. Am. Chem. Soc.* **2007**, *129*, 12688–12689. (d) Leitch, A. A.; Brusso, J. L.; Cvrkalj, K.; Reed, R. W.; Robertson, C. M.; Dube, P. A.; Oakley, R. T. *Chem. Commun.* **2007**, 3368–3370. (e) Leitch, A. A.; Reed, R. W.; Robertson, C. M.; Britten, J. F.; Yu, X.; Secco, R. A.; Oakley, R. T. *J. Am. Chem. Soc.* **2007**, *129*, 7903–7914.

(3) (a) Saito, G.; Yoshida, Y. *Bull. Chem. Soc. Jpn.* **2007**, *80*, 1–137. (b) Preuss, K. E. *Dalton Trans.* **2007**, 2357–2369. (c) Awaga, K.; Tanaka, T.; Shirai, T.; Umezono, Y.; Fujita, W. *C. R. Chim.* **2007**, *10*, 52–57. (d) Rawson, J. M.; Alberola, A.; Whalley, A. *J. Mater. Chem.* **2006**, *16*, 2560–2575. (e) Boere, R. T.; Roemmele, T. L. *Coord. Chem. Rev.* **2000**, *210*, 369–445. (f) Rawson, J. M.; MacManus, G. D. *Coord. Chem. Rev.* **1999**, *189*, 135–168.

(4) (a) Shuvaev, K. V.; Decken, A.; Grein, F.; Abeldin, T. M. S.; Thompson, L. K.; Passmore, J. *Dalton Trans.* **2008**, 4029–4037. (b) Cameron, T. S.; Decken, A.; Kowalczyk, R. M.; McInnes, E. J. L.; Passmore, J.; Rawson, J. M.; Shuvaev, K. V.; Thompson, L. K. *Chem. Commun.* **2006**, 2277–2279. (c) Decken, A.; Matar, S. M.; Passmore, J.; Shuvaev, K. V.; Thompson, L. K. *Inorg. Chem.* **2006**, *45*, 3878–3886. (d) Cameron, T. S.; Lemaire, M. T.; Passmore, J.; Rawson, J. M.; Shuvaev, K. V.; Thompson, L. K. *Inorg. Chem.* **2005**, *44*, 2576–2578.

(5) Hanson, P. *Adv. Heterocycl. Chem.* **1980**, *27*, 31–149.

Published on Web 07/15/2010

Chart 1

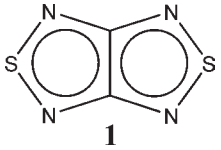

1

[1,2,5]thiadiazolo[3,4-*c*][1,2,5]thiadiazole (**1**; Chart 1), can be transformed into RAs with a number of reducing agents including early alkali metal (Li, Na, and K) and tris(dimethylamino)sulfonium thiophenolates, tetrakis(dimethylamino)ethene (TDAE), and $CoCp_2$ ($Cp = \eta^5$-C_5H_5). The RAs were isolated in the form of crystalline salts of corresponding cations and characterized by X-ray diffraction (XRD), and their magnetic properties were studied by experimental and theoretical methods.[6] In all cases, except $[TDAE]^{2+}[\mathbf{1}]^-_2$ featuring diamagnetic π dimers of the RAs, antiferromagnetic (AF) interactions in the salts' spin systems were observed.[6] These interactions were also found in some other 1,2,5-thiadiazolidyl-type RA salts, for example, in $[K(THF)]^+$-$[C_6H_4N_2S]^-$ (THF = tetrahydrofuran).[7] In all studied RA salts, including $[CoCp_2]^+[\mathbf{1}]^-$, the cations were diamagnetic; i.e., the salts were homospin ($S = {}^1/_2$).[6,7]

An interesting challenge is changing the character of magnetic interactions in the salts from AF to ferromagnetic (FM). The molecular design of FM π-heterocyclic RA salts is possible, in principle, with the McConnell I model[8] dealing with spin polarization (for a discussion of some other prospects, see ref9). To achieve a FM ground state, this model requires paramagnetic moieties of two types, with a positive spin density at one interacting with a negative spin density at another.[8] Because, according to available data, the spin density on the van der Waals (VdW) surfaces of the 1,2,5-thiadiazolidyl-type RAs is mostly positive,[9] paramagnetic cations with peripheral negative spin density are necessary as counterions. Such cations are known to be, for example, $[MCp^*_2]^+$ [M = Cr, Mn, Fe; Cp* = η^5-$C_5(CH_3)_5$].[10]

It is believed that the McConnell I mechanism stands behind the FM properties of a number of the $[MCp^*_2]^+$-$[TCNE]^-$ and $[MCp^*_2]^+[TCNQ]^-$ salts, with $T_C = 8.8$ K for $[MnCp^*_2]^+[TCNE]^-$.[10−13] At the same time, it should be emphasized that creation of the FM ground state with the McConnell I model critically depends on the crystal packing of the target salt (mutual orientation and spatial proximity of fragments with required spin polarization), i.e., on property that can hardly be a priori predicted and/or controlled.[14] For the aforementioned $[TCNE]^-$ and $[TCNQ]^-$ salts' polymorphs (where known), the typical situation is that only one has FM properties, whereas the others do not.[11−13] Some other structural problems are illustrated by the fact that nonstoichiometric salt $[V^{II}]^{2+}[TCNE]^-_z[TCNE]^{2-}_{1-z/2}$ ($1 < z < 2$), whose T_C exceeds room temperature, is a noncrystalline kinetic phase, whereas the crystalline phase is not a magnetically ordered material.[15]

In this work, we report the reduction of compound **1** with $CrCp^*_2$ (**2**) and the XRD structure and magnetic properties of the RA salt $[\mathbf{2}]^+[\mathbf{1}]^-$ (**3**) obtained.

Experimental and Computational Details

General Procedures. All operations were carried out under argon; in the synthesis and manipulation of salt **3**, the glovebox and Schlenk techniques were used. Compound **2** was received from Dalchem and additionally purified by crystallization from hexane. All solvents were distilled under argon with common drying agents.

Syntheses. Compound 1. A solution of 3-chloro-4-fluoro-1,2,5-thiadiazole[16] (2.77 g, 0.02 mol) and $(Me_3SiN{=})_2S$[17f] (4.12 g, 0.02 mol) in absolute MeCN (25 mL) was added dropwise, for 30 min, to a refluxed and stirred suspension of freshly calcinated CsF (6.08 g, 0.04 mol) in MeCN (75 mL). After an additional 30 min, the reaction mixture was cooled to 20 °C and filtered, and the solvent was distilled off under reduced pressure. The residue was chromatographed on a silica column with hexane, the solvent evaporated, and the residual solid sublimed in vacuo and recrystallized from hexane. Compound **1**[6e] was obtained as long colorless needles [1.67 g (58%), mp 117−118 °C].

Compound 3. The reaction was carried out in an H-shaped Schlenk vessel. A solution of **1** (21.3 mg, 0.15 mmol) in THF (1 mL) was placed into one tube and a solution of **2** (47.6 mg, 0.15 mmol) in THF (1 mL) into the other tube. Then pure THF was gently layered over both solutions up to the middle level of the horizontal tube (ca. 30 mL in total). The reaction vessel was kept at ambient temperature over 3 weeks. Salt **3** formed red-brown crystals suitable for XRD [yield 67 mg (97%), mp (sealed capillary) > 300 °C]. Calcd for $C_{22}H_{30}CrN_4S_2$: C, 56.62; H, 6.48; N, 12.01. Found: C, 56.60; H, 6.15; N, 11.90.

Crystallographic Analysis. The XRD data for salt **3** were collected with a Bruker X8Apex diffractometer with Mo Kα ($\lambda = 0.710\,73$ Å) radiation and a graphite monochromator. The

(6) (a) Konchenko, S. N.; Gritsan, N. P.; Lonchakov, A. V.; Irtegova, I. G.; Mews, R.; Ovcharenko, V. I.; Radius, U.; Zibarev, A. V. *Eur. J. Inorg. Chem.* **2008**, 3833–3838. (b) Gritsan, N. P.; Lonchakov, A. V.; Lork, E.; Mews, R.; Pritchina, E. A.; Zibarev, A. V. *Eur. J. Inorg. Chem.* **2008**, 1994–1998. (c) Bagryanskaya, I. Yu.; Gatilov, Yu. V.; Gritsan, N. P.; Ikorskii, V. N.; Irtegova, I. G.; Lonchakov, A. V.; Lork, E.; Mews, R.; Ovcharenko, V. I.; Semenov, N. A.; Vasilieva, N. V.; Zibarev, A. V. *Eur. J. Inorg. Chem.* **2007**, 4751–4761. (d) Ikorskii, V. N.; Irtegova, I. G.; Lork, E.; Makarov, A. Yu.; Mews, R.; Ovcharenko, V. I.; Zibarev, A. V. *Eur. J. Inorg. Chem.* **2006**, 3061–3067. (e) Makarov, A. Yu.; Irtegova, I. G.; Vasilieva, N. V.; Bagryanskaya, I. Yu.; Borrmann, T.; Gatilov, Yu. V.; Lork, E.; Mews, R.; Stohrer, W.-D.; Zibarev, A. V. *Inorg. Chem.* **2005**, *44*, 7194–7199.

(7) (a) Bogomyakov, A. S.; Semenov, N. A.; Pushkarevskii, N. A. Unpublished results, **2009** (experimental magnetic structure featuring AF interactions). (b) Konchenko, S. N.; Gritsan, N. P.; Lonchakov, A. V.; Radius, U.; Zibarev, A. V. *Mendeleev Commun.* **2009**, *19*, 7–9(XRD and theoretical magnetic structure featuring both AF and FM interactions).

(8) (a) Novoa, J. J.; Deumal, M. *Struct. Bonding (Berlin)* **2001**, *100*, 33–60. (b) Kahn, O. *Molecular Magnetism*; VCH Publishers: New York, 1993; p 380. (c) McConnell, H. M. *J. Chem. Phys.* **1963**, *39*, 1910–1917.

(9) Vasilieva, N. V.; Irtegova, I. G.; Gritsan, N. P.; Lonchakov, A. V.; Makarov, A. Yu.; Shundrin, L. A.; Zibarev, A. V. *J. Phys. Org. Chem.* **2010**, *23*, 536–543.

(10) (a) Kaupp, M.; Koehler, F. H. *Coord. Chem. Rev.* **2009**, *253*, 2376–2386. (b) Heise, H.; Koehler, F. H.; Herker, M.; Hiller, W. *J. Am. Chem. Soc.* **2002**, *124*, 10823–10832. (c) Kollmar, C.; Kahn, O. *J. Chem. Phys.* **1992**, *96*, 2988–2997.

(11) (a) Miller, J. S. *J. Mater. Chem.* **2010**, *20*, 1846–1857. (b) Her, J. H.; Stephens, P. W.; Ribas-Arino, J.; Novoa, J. J.; Shum, W. W.; Miller, J. S. *Inorg. Chem.* **2009**, *48*, 3296–3307. (c) Miller, J. S. *Dalton Trans.* **2006**, 2742–2749. (d) Miller, J. S. *Adv. Mater.* **2002**, *14*, 1105–1110. (e) Miller, J. S. *Inorg. Chem.* **2002**, *39*, 4392–4408. (f) Miller, J. S.; Epstein, A. J. *Angew. Chem., Int. Ed.* **1994**, *33*, 385–415. (g) Miller, J. S.; Epstein, A. J.; Reiff, M. W. *Chem. Rev.* **1988**, *88*, 201–220.

(12) (a) Broderick, W. E.; Eichhorn, D. M.; Liu, X.; Toscano, P. J.; Owens, S. M.; Hoffman, B. M. *J. Am. Chem. Soc.* **1995**, *117*, 3641–3642. (b) Eichhorn, D. M.; Skee, D. C.; Broderick, W. E.; Hoffman, B. M. *Inorg. Chem.* **1993**, *32*, 491–492. (c) Broderick, W. E.; Hoffman, B. M. *J. Am. Chem. Soc.* **1991**, *113*, 6334–6335.

(13) Koizumi, K.; Shoji, M.; Ritawaga, Y.; Takeda, R.; Yamanaka, S.; Kawakami, T.; Okumura, M.; Yamaguchi, K. *Polyhedron* **2007**, *26*, 2135–2141.

(14) Price, S. L. *Acc. Chem. Res.* **2009**, *42*, 117–126.

(15) Miller, J. S. *Polyhedron* **2009**, *28*, 1596–1605.

(16) Geisel, M.; Mews, R. *Chem. Ber.* **1982**, *115*, 2135–2140.

structure was solved by direct methods and refined by a full-matrix least-squares method on F^2 in the anisotropic (isotropic for H atoms) approximation implemented in the *SHELXL-97* program.[18] All H atoms were located geometrically. The obtained crystal structure was analyzed for short contacts between nonbonded atoms by means of the *PLATON*[19] and *MERCURY*[20] programs: $C_{22}H_{30}CrN_4S_2$, M = 466.64, monoclinic, space group $P2_1/c$, a = 8.7270(4) Å, b = 27.2622(16) Å, c = 9.5584(5) Å, β = 94.869(2)°, V = 2265.9(2) Å^3, T = 120 K, Z = 4, ρ_{calcd} = 1.368 g·cm^{-1}, μ(Mo Kα) = 0.705 mm^{-1}, crystal size 0.53 × 0.40 × 0.13 mm, reflections measured 2 1628 [6285 unique, 4888 with $I \geq 2\sigma(I)$], R_{int} = 0.0348, no. of parameters = 272, R1 = 0.0438 [for $I \geq 2\sigma(I)$], wR2 = 0.1152 (all reflections), $\Delta\rho_{min,max}$ = −0.56, +0.46 e·Å^{-3}, GOF = 1.162. CCDC 772046 contains the supplementary crystallographic data for this paper. These data can be obtained free of charge from the Cambridge Crystallographic Data Centre via www.ccdc.cam.ac.uk/data_request/cif.

Magnetic Measurements. The magnetic susceptibility measurements on salt **3** were performed with an MPMS-XL Quantum Design SQUID magnetometer in the temperature range 2−300 K in the magnetic fields of 500, 1000, 3000, and 5000 Oe. Invariance to the field evidenced the absence of FM impurities in the sample. The molar magnetic susceptibility χ of salt **3** was calculated using the standard diamagnetism corrections.[21] The effective magnetic moment of the salt (μ_{eff}) was calculated by eq 1:

$$\mu_{eff} = \left(\frac{3k}{N\beta^2}\chi T\right)^{1/2} \approx (8\chi T)^{1/2} \quad (1)$$

Scheme 1

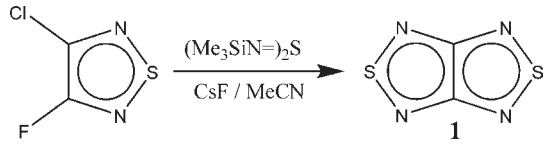

1

Quantum Chemical Calculations. Unless otherwise indicated, the *Gaussian03* set of programs[22] was used in the calculations. The theoretical analysis of the magnetic structure of the salt **3** was based on the Heisenberg Hamiltonian (2).[8a,b]

$$\hat{H} = -2\sum_{i,j}^{N} J_{ij}\vec{S}_i\vec{S}_j \quad (2)$$

Within this formalism, the parameters of the pair exchange interactions (J_{ij}) were calculated using the energy splitting ($\Delta E_{LH} = E_L - E_H$) between the low-spin ($S_{min} = S_1 - S_2$) and high-spin ($S_{max} = S_1 + S_2$) states of the pairs of paramagnetic species (3).

$$J = \frac{\Delta E_{LH}}{2} \quad \text{for } S_1 = S_2 = \frac{1}{2}$$
$$J = \frac{\Delta E_{LH}}{4} \quad \text{for } S_1 = \frac{3}{2},\ S_2 = \frac{1}{2} \quad (3)$$
$$J = \frac{\Delta E_{LH}}{12} \quad \text{for } S_1 = S_2 = \frac{3}{2}$$

The most accurate and straightforward way to evaluate the ΔE_{LH} values is to use the CASSCF procedure[23] for the calculations. The active space for the CASSCF calculations was selected to allow a proper description of the electronic structure and energy of the high- and low-spin states of the pairs. The energy splitting for the $[\mathbf{1}]^-\cdots[\mathbf{2}]^+$ pairs was calculated at the CASSCF(8,8) level. The active space includes five d orbitals of the chromium center, two occupied π orbitals of $C_5(CH_3)_5$ ligands that interact with the d_{xz} and d_{yz} orbitals of the Cr atom (Figure 4), and the π-SOMO (singly occupied molecular orbital) of $[\mathbf{1}]^-$.[6] The energy splitting for the $[\mathbf{2}]^+\cdots[\mathbf{2}]^+$ pair was calculated at the CASSCF(14,14) level with the aforementioned set of seven orbitals for each $[\mathbf{2}]^+$. The energy splitting for the $[\mathbf{1}]^-\cdots[\mathbf{1}]^-$ pairs was computed at the CASSCF(10,10) level with the active space constructed from four occupied π-MOs, two π-SOMOs, and four vacant π^*-MOs of two $[\mathbf{1}]^-$.[6] All calculations of the pair exchange interactions were performed for the XRD crystal structure of salt **3** (Figures 2 and 5).

The CASSCF calculations were done using Ahlrichs' TZV basis set on the Cr atom, the 6-31G(d) basis set on Cp* ligands, and the 6-31+G(d) basis set on C, N, and S atoms of $[\mathbf{1}]^-$.

The exchange parameters J were also calculated using the broken-symmetry (BS) approach[24] at the UB3LYP or UPBE0 levels of theory. For $[\mathbf{1}]^-\cdots[\mathbf{1}]^-$ pairs, both levels were employed and the 6-31+G(d) basis set was used. Calculations for $[\mathbf{1}]^-\cdots[\mathbf{2}]^+$ pairs were performed only at the UPBE0 level with the 6-31G basis set. For the $[\mathbf{2}]^+\cdots[\mathbf{2}]^+$ pair, the UPBE0 calculations with the Def2-TZVP(-df) basis set[25] for the Cr atom and the Def2-SV(P) basis set[26] for other atoms were

(17) (a) Blockhuys, F.; Gritsan, N. P.; Makarov, A. Yu.; Tersago, K.; Zibarev, A. V. *Eur. J. Inorg. Chem.* **2008**, 655–672. (b) Makarov, A. Yu.; Tersago, K.; Nivesanond, K.; Blockhuys, F.; Van Alsenoy, C.; Kovalev, M. K.; Bagryanskaya, I. Yu.; Gatilov, Yu. V.; Shakirov, M. M.; Zibarev, A. V. *Inorg. Chem.* **2006**, *45*, 2221–2228. (c) Makarov, A. Yu.; Bagryanskaya, I. Yu.; Blockhuys, F.; Van Alsenoy, C.; Gatilov, Yu. V.; Knyazev, V. V.; Maksimov, A. M.; Mikhalina, T. V.; Platonov, V. E.; Shakirov, M. M.; Zibarev, A. V. *Eur. J. Inorg. Chem.* **2003**, 77–88. (d) Lork, E.; Mews, R.; Shakirov, M. M.; Watson, P. G.; Zibarev, A. V. *J. Fluorine Chem.* **2002**, *115*, 165–168. (e) Lork, E.; Mews, R.; Shakirov, M. M.; Watson, P. G.; Zibarev, A. V. *Eur. J. Inorg. Chem.* **2001**, 2123–2134. (f) Bagryanskaya, I. Yu.; Gatilov, Yu. V.; Miller, A. O.; Shakirov, M. M.; Zibarev, A. V. *Heteroatom Chem.* **1994**, *5*, 561–565. (g) Zibarev, A. V.; Gatilov, Yu. V.; Miller, A. O. *Polyhedron* **1992**, *11*, 1137–1141. (h) Zibarev, A. V.; Miller, A. O. *J. Fluorine Chem.* **1990**, *50*, 359–563.

(18) Sheldrick, G. M. *SHELX-97: Programs for Crystal Structure Analysis*, release 97-2; University of Goettingen: Goettingen, Germany, 1997.

(19) (a) Spek, A. L. *PLATON, A Multipurpose Crystallographic Tool*, version 10M; Utrecht University: Utrecht, The Netherlands, 2003. (b) Spek, A. L. *J. Appl. Crystallogr.* **2003**, *36*, 7–13.

(20) Macrae, C. F.; Edgington, P. R.; McCabe, P.; Pidcock, E.; Shields, G. P.; Taylor, R.; Towler, J.; van de Stree, M. *J. Appl. Crystallogr.* **2006**, *39*, 453–457.

(21) Kalinnikov, V. T.; Rakitin, Yu. V. *Introduction in Magnetochemistry. Method of Static Magnetic Susceptibility*; Nauka: Moscow, 1980; p 302 (in Russian).

(22) Frisch, M. J.; Trucks, G. W.; Schlegel, H. B.; Scuseria, G. E.; Robb, M. A.; Cheeseman, J. R.; Montgomery, J. J. A.; Vreven, T.; Kudin, K. N.; Burant, J. C.; Millam, J. M.; Iyengar, S. S.; Tomasi, J.; Barone, V.; Mennucci, B.; Cossi, M.; Scalmani, G.; Rega, N.; Petersson, G. A.; Nakatsuji, H.; Hada, M.; Ehara, M.; Toyota, K.; Fukuda, R.; Hasegawa, J.; Ishida, M.; Nakajima, T.; Honda, Y.; Kitao, O.; Nakai, H.; Klene, M.; Li, X.; Knox, J. E.; Hratchian, H. P.; Cross, J. B.; Bakken, V.; Adamo, C.; Jaramillo, J.; Gomperts, R.; Stratmann, R. E.; Yazyev, O.; Austin, A. J.; Cammi, R.; Pomelli, C.; Ochterski, J. W.; Ayala, P. Y.; Morokuma, K.; Voth, G. A.; Salvador, P.; Dannenberg, J. J.; Zakrzewski, V. G.; Dapprich, S.; Daniels, A. D.; Strain, M. C.; Farkas, O.; Malick, D. K.; Rabuck, A. D.; Raghavachari, K.; Foresman, J. B.; Ortiz, J. V.; Cui, Q.; Baboul, A. G.; Clifford, S.; Cioslowski, J.; Stefanov, B. B.; Liu, G.; Liashenko, A.; Piskorz, P.; Komaromi, I.; Martin, R. L.; Fox, D. J.; Keith, T.; Al-Laham, M. A.; Peng, C. Y.; Nanayakkara, A.; Challacombe, M.; Gill, P. M. W.; Johnson, B.; Chen, W.; Wong, M. W.; Gonzalez, C.; Pople, J. A. *Gaussian03*, revision E.01; Gaussian, Inc.: Wallingford, CT, 2004.

(23) Ross, B. O. *Adv. Chem. Phys.* **1987**, *69*, 339–445.

(24) (a) Nagao, H.; Nishino, M.; Shigeta, Y.; Soda, T.; Kitagawa, Y.; Onishi, T.; Yoshika, Y.; Yamaguchi, K. *Coord. Chem. Rev.* **2000**, *198*, 265–295. (b) Noodleman, L.; Case, D. A.; Mouesca, J. M. *Coord. Chem. Rev.* **1995**, *144*, 199–244. (c) Noodleman, L.; Davidson, E. R. *Chem. Phys.* **1986**, *109*, 131–143. (d) Noodleman, L. *J. Chem. Phys.* **1981**, *74*, 5737–5743.

(25) Schaefer, A.; Horn, H.; Ahlrichs, R. *J. Chem. Phys.* **1992**, *97*, 2571–2577.

(26) Weigend, F.; Ahlrichs, R. *Phys. Chem. Chem. Phys.* **2005**, *7*, 3297–3305.

Scheme 2

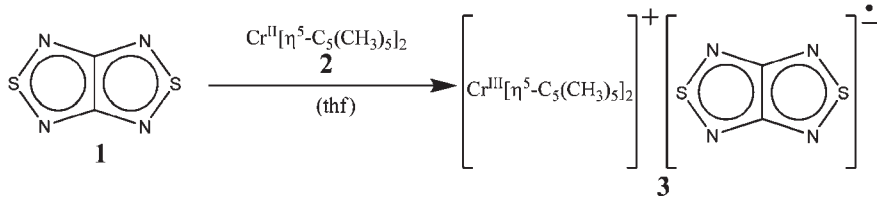

carried out using the *ORCA* program package.[27] The J values were obtained from the formula (4)[28]

$$J = -\frac{E^{HS} - E^{LS}_{BS}}{\langle S^2\rangle^{HS} - \langle S^2\rangle^{LS}_{BS}} \quad (4)$$

where E^{HS} is the energy of the high-spin state of the pair and E^{LS}_{BS} is the energy of the low-spin state within the BS approach.[24] The accuracy of the energy calculations was chosen to be 10^{-8} H, which provided calculations of the J values with an accuracy of 0.004 cm^{-1}.

Magnetic Property Simulations. Because the exchange interaction between $[\mathbf{1}]^-$ and $[\mathbf{2}]^+$ in the crystal of **3** is negligible (see the next section), the molar magnetic susceptibility, $\chi(T)$ (Figure 3), is the sum of the contributions from the $\{[\mathbf{1}]^-\cdots[\mathbf{1}]^-\}$ and $\{[\mathbf{2}]^+\cdots[\mathbf{2}]^+\}$ sublattices. A small fraction of paramagnetic impurities presents usually in the samples. Thus, the molar magnetic susceptibility of the sample of the salt **3** can be approximated by the formula (5)

$$\chi(T) = \frac{1}{2}[\chi_1(T) + \chi_2(T)](1-p) + \frac{N\beta^2 g^2}{4kT}p \quad (5)$$

where $\chi_1(T)$ is the molar magnetic susceptibility of the $\{[\mathbf{1}]^-\cdots[\mathbf{1}]^-\}$ sublattice, $\chi_2(T)$ is the molar magnetic susceptibility of the $\{[\mathbf{2}]^+\cdots[\mathbf{2}]^+\}$ sublattice, and p is a contribution from the paramagnetic impurity with $S = {}^1/_2$. Consequently, $\chi_1(T)$ was calculated for the sample consisting of dimers of spins $S = {}^1/_2$ using the formula of Bleaney and Bowers (6)[29] and $\chi_2(T)$ for the sample consisting of dimers of spins $S = {}^3/_2$ using formula (7), which could be easily derived from the general formula deduced by Van Vleck.[8b]

$$\chi_1 = \frac{2Ng^2{\mu_B}^2}{kT}\frac{1}{3+\exp\left(-\frac{2J}{kT}\right)} \quad (6)$$

$$\chi_2 = \frac{2Ng^2{\mu_B}^2}{kT}\frac{\exp\left(\frac{2J}{kT}\right) + 5\exp\left(\frac{2J}{kT}\right) + 14\exp\left(\frac{2J}{kT}\right)}{1+3\exp\left(\frac{2J}{kT}\right) + 5\exp\left(\frac{6J}{kT}\right) + 7\exp\left(\frac{12J}{kT}\right)} \quad (7)$$

The theoretical temperature dependence of the effective magnetic moment, $\mu_{eff}(T)$ (Figure 3), was calculated using formula (1) with $\chi(T)$ from formula (5).

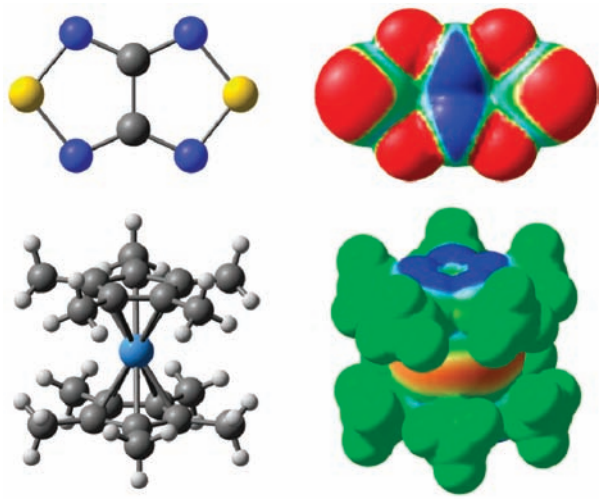

Figure 1. Spin-density distribution at the VdW surfaces (right column, sign color code: red, $> 4 \times 10^{-4}$; blue, $< -4 \times 10^{-4}$; green, zero) of $[\mathbf{1}]^-$ (top) and $[\mathbf{2}]^+$ (bottom) from UB3LYP/6-31+G(d) calculations. Color code for the chemical structures (left column): yellow, S; blue, N; gray, C; light blue, Cr; light gray, H.

Results and Discussion

In previous work,[6e] compound **1** was synthesized by a condensation/cyclization reaction between 3,4-difluoro-1,2,5-thiadiazole and $(Me_3SiN{=})_2S$ induced by CsF. In this work, 3-chloro-4-fluoro-1,2,5-thiadiazole was successfully used for the preparation of **1** in an isolated yield of 58% (Scheme 1), which gave the first example of chlorine substitution in a whole family of these types of reactions, both intra- and intermolecular.[17] Preliminary substitution of Cl by F in the precursor requires very drastic reaction conditions.[16]

According to the DFT calculations,[30] derivatives of the 1,2,5-chalcogenadiazole ring system (chalcogen: S, Se) normally possess positive electron affinity (EA), which means that their RAs are thermodynamically more stable than neutral molecules.[31] For compound **1**, adiabatic EA is 2.14 eV at the (U)B3LYP/6-31+G(d) level of theory. As mentioned above, this compound can be readily reduced into its RA with a number of reducing agents including $CoCp_2$,[6] whose He^I UPS ionization energy (IE_1) is 5.56 eV.[32] Consequently, other organometallics with comparable IE_1 values should also reduce compound **1**.

Indeed, with THF as the solvent and at ambient temperature, decamethylchromocene **2** (He^I UPS, IE_1 = 4.93 eV)[32] readily reduced compound **1** with formation of the $[\mathbf{2}]^+[\mathbf{1}]^-$ salt (**3**; Scheme 2) in practically quantitative yield. The salt **3**

(27) (a) Neese, F. *ORCA—An Ab Initio, Density Functional and Semiempirical Program Package*, version 2.7.0β; University of Bonn: Bonn, Germany, 2009. (b) Neese, F. *J. Phys. Chem. Solids* **2004**, *65*, 781–785.

(28) (a) Soda, T.; Kitagawa, Y.; Onishi, T.; Takano, T.; Shigeta, Y.; Nagao, H.; Yoshioka, Y.; Yamaguchi, K. *Chem. Phys. Lett.* **2000**, *319*, 223–230. (b) Yamaguchi, K.; Takahara, Y.; Fueno, T. In *Applied Quantum Chemistry*; Smith, V. H., Ed.; Reidel: Dordrecht, The Netherlands, 1986; p 155.

(29) Bleaney, B.; Bowers, K. D. *Proc. R. Soc. London, Ser. A* **1952**, *214*, 451–465.

(30) Gritsan, N. P.; Lonchakov, A. V.; Zibarev, A. V. Work in progress.

(31) Rienstra-Kiracofe, J. C.; Tschumper, G. S.; Shaefer, H. F.; Nandi, S.; Ellison, G. B. *Chem. Rev.* **2002**, *102*, 231–282.

(32) Green, J. C. *Struct. Bonding* (*Berlin*) **1986**, *43*, 37–112.

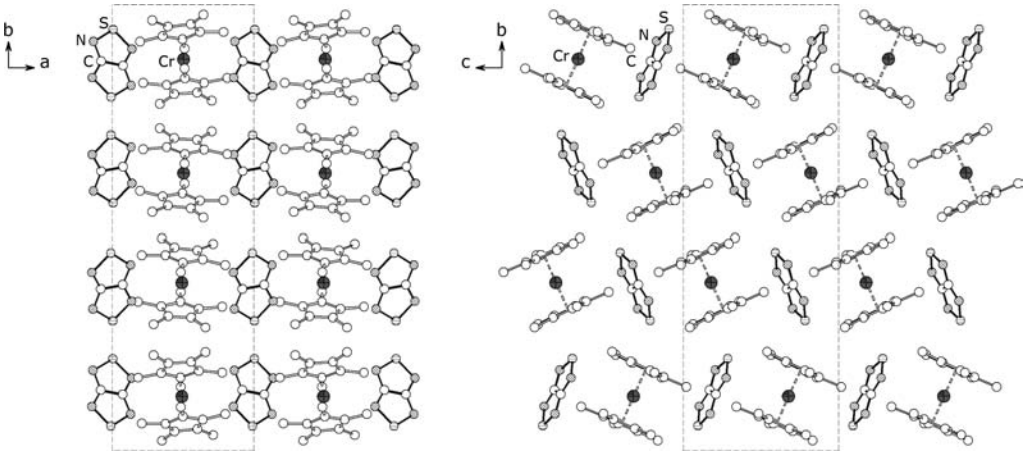

Figure 2. Crystal structure of the salt **3**. Selected bond lengths (Å) and angles (deg) in the RA $[\mathbf{1}]^-$ (chemical numbering used): S1−N1 1.662(3), S1−N2 1.657(2), S2−N3 1.661(3), S2−N4 1.658(3), N1−C1 1.336(3), N2−C2 1.338(3), N3−C1 1.340(3), N4−C2 1.333(4), C1−C2 1.454(4); N1−S1−N2 101.50(12), N3−S2−N4 101.59(13), S1−N1−C1 104.54(19), S1−N2−C2 104.60(16), S2−N3−C1 104.4(2), S2−N4−C2 104.6(2), N1−C1−N3 130.7(3), N1−C1−C2 114.7(2), N3−C1−C2 114.6(2), N2−C2−N4 130.5(2), N2−C2−C1 114.7(2), N4−C2−C1 114.8(2).

is air-sensitive and is decomposed by atmospheric moisture (cf. ref 33).

At the same time, decamethylferrocene (IE_1 = 5.88 eV)[32] does not reduce compound **1** in THF under refluxing.

In the salt **3**, the cation $[\mathbf{2}]^+$ is an $S = {}^3/_2$ paramagnetic species and the anion $[\mathbf{1}]^-$ is an $S = {}^1/_2$ paramagnetic species. At the same time at room temperature and with a conventional X-band electron spin resonance (ESR) technique, the salt **3** is ESR-silent in both the solid state and a MeCN solution. This can be associated with the huge zero-field splitting and fast relaxation of the cation[34] provoking fast relaxation of the anion; in solution, the salt exists very likely in the form of an ion-pair typical of these types of RAs.[5,35] For previously studied salt $[CoCp_2]^+[\mathbf{1}]^-$ with a diamagnetic cation, the ESR signals were observed in both phases.[6a]

The spin density at VdW surfaces of $[\mathbf{1}]^-$ and $[\mathbf{2}]^+$ ions was calculated at the UB3LYP/6-31+G(d) level of theory (Figure 1). It is seen that the spin density at the VdW surface of $[\mathbf{1}]^-$ is mostly positive, however, with an island of negative spin density in the vicinity of the C−C bond. On the contrary, the spin density at the VdW surface of $[\mathbf{2}]^+$ is mostly close to zero with an island of negative spin density in the vicinity of the C_5 ring. The magnetic properties of the salt are therefore controlled by the way in which these ions are packed in the crystal.

The structure of the salt **3** from single-crystal XRD is shown in Figure 2. The geometry of $[\mathbf{1}]^-$ is very similar to that in its salts isolated previously:[6] the bond lengths coincide within 0.01 Å and the bond angles within 0.2°. In the crystal of salt **3**, the ions form a layered structure with alternating cationic and anionic layers shifted by $x/2$ along the a axis. As a consequence, the anions are displaced in the pits of the cationic layer, and vice versa. The structure reveals a stacked orientation of two neighboring cations whose separation of 3.77 Å exceeds, however, the sum of the VdW radii of the C atoms of 3.54 Å;[36] the Cr···Cr separation is 7.49 Å. This structure of salt **3** is very different from that of $[MCp^*_2]^+$-$[TCNE]^-$ (M = Cr, Mn, Fe) salts featuring in all cases parallel chains of alternating cations (donors, D^+) and anions (acceptors, A^-), $\cdots D^+A^-D^+A^-\cdots$, with interchain M···M separations of 10.7 ± 0.3 Å.[11] The crystal packing of **3** is also different from that of salt $[CoCp_2]^+[\mathbf{1}]^-$, where cations and anions form zigzag chains; neighboring $[\mathbf{1}]^-$ reveals S···N contacts slightly exceeding the sum of the VdW radii.[6a]

Experimental magnetic properties of the salt **3** in the temperature range 2−300 K are presented in Figure 3. The effective magnetic moment (μ_{eff}) of the salt increases with temperature. At 300 K, its value of 4.27 μ_B is close to the spin-only value of 4.24 μ_B for an uncorrelated randomly oriented two-spin system with $S = {}^3/_2$ and ${}^1/_2$ and $g = 2$ for both spins. The g value of $[\mathbf{1}]^-$ was measured previously as 2.0045.[6] Our UB3LYP/6-311+G(d,p) calculations predict for $[\mathbf{2}]^+$ in its XRD geometry (Figure 2) an almost isotropic g value as g_{xx} = 1.954, g_{yy} = 1.955, g_{zz} = 1.988, and g_{iso} = 1.966. It is well-known that the chromocenium cation, the archetype of $[\mathbf{2}]^+$, has a nondegenerate ground state and, thus, a pure spin magnetic moment.[34] The selected MOs of $[\mathbf{2}]^+$ calculated at the ROHF level are shown in Figure 4.

The magnetic susceptibility (χ) of the salt **3** increases steadily with a lowering of the temperature (Figure 3). The reciprocal χ obeys the Curie−Weiss law between 300 and 50 K and then deviates from linearity. Extrapolation of the linear part onto axis T gives a negative Weiss constant of ca. −10 K. Thus, $\mu_{eff}(T)$, $\chi(T)$, and $\chi^{-1}(T)$ dependences altogether evidence AF interactions in the salt's spin system. Comparing Figures 1 and 2, one can assume that the crystal packing of **3** is really not well-suited to contact between the paramagnetic ions satisfying the McConnell I model.

To interpret the experimental magnetic properties of the salt **3** in detail, theoretical analysis of the pair exchange interactions in its crystal was performed. To calculate the pair exchange interactions, we used both the CASSCF[23] and spin-unrestricted BS[24] approaches. We demonstrated previously[6] that the BS approach, in combination with the DFT method,[37]

(33) Lork, E.; Mews, R.; Zibarev, A. V. *Mendeleev Commun.* **2009**, *19*, 147–148.

(34) (a) Solodovnikov, S. P. *Russ. Chem. Rev.* **1982**, *51*, 961–974. (b) Warren, K. D. *Struct. Bonding* (*Berlin*) **1976**, *27*, 45–159.

(35) (a) Bock, H.; Haenel, P.; Neidlein, R. *Phosphorus Sulfur Relat. Elem.* **1988**, *39*, 235–252. (b) Kwan, C. L.; Carmack, M.; Kochi, J. K. *J. Phys. Chem.* **1976**, *80*, 1786–1792.

(36) Rowland, R. S.; Taylor, R. *J. Phys. Chem.* **1996**, *100*, 7384–7391.

(37) (a) Neese, F. *Coord. Chem. Rev.* **2009**, *253*, 526–563. (b) Geerling, P.; De Proft, F.; Langenaeker, W. *Chem. Rev.* **2003**, *103*, 1793–1873.

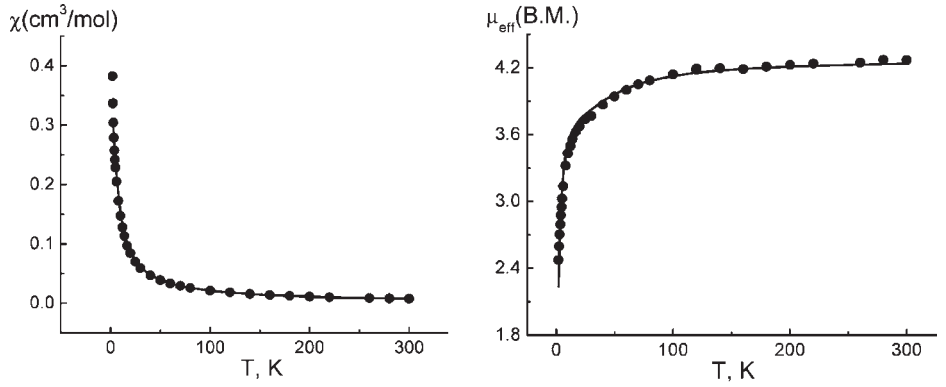

Figure 3. Experimental temperature dependences (dots) of the magnetic susceptibility χ (left) and effective magnetic moment μ_{eff} (right) for the salt **3** in the temperature range 2−300 K. The solid curves are the best fits obtained using formulas (5)−(7) (see the Experimental Section). The fitting parameters are the following: $J_1 = -40 \pm 9$ cm^{-1}, $J_2 = -0.58 \pm 0.03$ cm^{-1}, and $p = 1.7 \pm 0.4\%$.

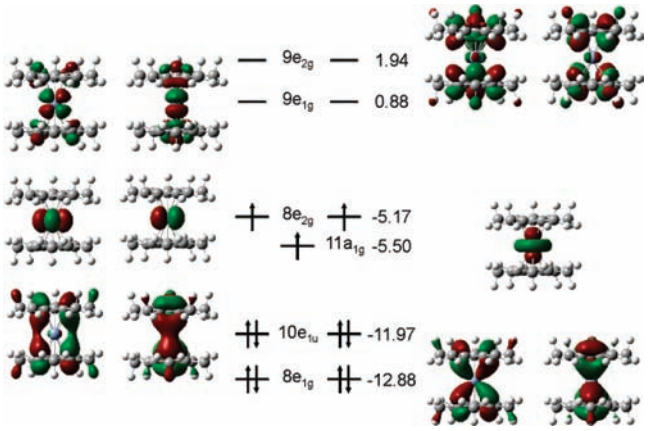

Figure 4. Molecular orbitals and their energies (eV) calculated for the $^4A_{1g}$ ground state of the cation $[\mathbf{2}]^+$ at the ROHF/6-31G(d) level. The structure constrained to D_{5d} symmetry was optimized at the UB3LYP level.

describes fairly well the exchange interaction between RAs $[\mathbf{1}]^-$ in a number of crystal structures.

In the case of **3**, three types of pairs, namely, $[\mathbf{1}]^-\cdots[\mathbf{1}]^-$, $[\mathbf{2}]^+\cdots[\mathbf{2}]^+$, and $[\mathbf{1}]^-\cdots[\mathbf{2}]^+$, should be taken into account in exchange calculations. In the crystal of **3**, five unique $[\mathbf{1}]^-\cdots[\mathbf{1}]^-$ pairs with S···S distances within 10 Å, varying from 3.52 to 8.76 Å, can be identified (Figure 5). The minimal S···S distance is slightly shorter than the sum of the VdW radii of 3.62 Å.[36] The calculated J values for the $[\mathbf{1}]^-\cdots[\mathbf{1}]^-$ pairs are given in Table 1. It is seen that both approaches predict that the J value for pair 1 (featuring the shortest S···S distance) is significantly larger than all of the others (Table 1 and Figure 5), although the value obtained with the CASSCF method is 4 times smaller than that obtained with the BS approach.

For eight unique $[\mathbf{1}]^-\cdots[\mathbf{2}]^+$ pairs with a separation within 10 Å (Figure 5), J values calculated using the BS approach at the UPBE0 level were both positive (FM) and negative (AF) and lying in the range −200 to +200 cm^{-1}, i.e., nonrealistically large (Supporting Information, Table S1). With the CASSCF approach, however, only very weak FM and AF interactions with J values in the range −0.14 to +0.08 cm^{-1} were predicted (Table 2).

The J values for the $[\mathbf{2}]^+\cdots[\mathbf{2}]^+$ pair were predicted as −0.08 cm^{-1} at the CASSCF(14,14)/6-31G(d) level and −0.33 and −0.28 cm^{-1} at the BS UPBE0 and UB3LYP levels, respectively.

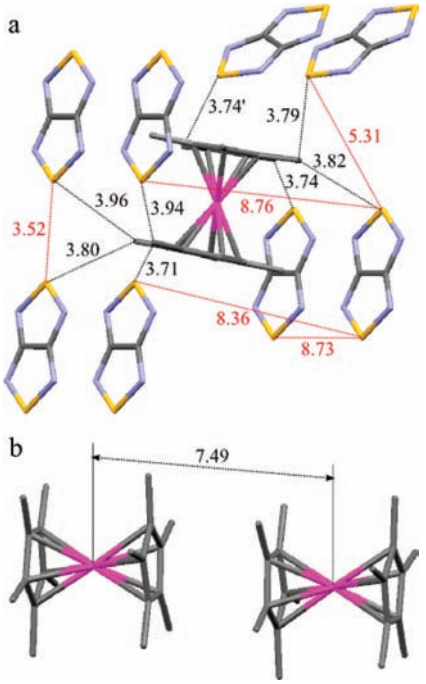

Figure 5. Ion pairs included in the calculations of the exchange interactions (contact distances in Å): (a) five unique $[\mathbf{1}]^-\cdots[\mathbf{1}]^-$ pairs (red contacts) and eight unique $[\mathbf{1}]^-\cdots[\mathbf{2}]^+$ pairs (blue contacts); (b) the $[\mathbf{2}]^+\cdots[\mathbf{2}]^+$ pair.

Table 1. Exchange Interaction Parameters (J) for the $[\mathbf{1}]^-\cdots[\mathbf{1}]^-$ Pairs (Figure 5) Calculated at Various Levels of Theory

		J, cm^{-1}	
pair	contact distance, Å	BS UB3LYP/ 6-31+G(d)	CASSCF(10,10)/ 6-31+G(d)
1	3.52	−61.0	−15.3
2	5.31	−0.77	0.12
3	8.36	~0	~0
4	8.73	0	0
5	8.76	−0.07	~0

Thus, the FM interactions between $[\mathbf{1}]^-$ and $[\mathbf{2}]^+$ in the crystal of **3**, satisfying the McConnell I model, belong to the weakest among theoretically calculated exchange interactions.

Overall, the calculations revealed rather a simple magnetic structure of the salt **3**. When very small exchange interactions are neglected, the structure can be considered as a set of two

Table 2. Exchange Interaction Parameters (J) for the $[\mathbf{1}]^-\cdots[\mathbf{2}]^+$ Pairs (Figure 5) Calculated at the CASSCF(8,8) Level of Theory[a]

pair	contact distance, Å	J, cm^{-1}
1	3.71	−0.02
2	3.74	0.08
3	3.74	−0.12
4	3.79	−0.14
5	3.80	−0.01
6	3.82	−0.02
7	3.94	0.08
8	3.96	−0.05

[a] The following basis sets were used in the calculations: TZV for the Cr atom and 6-31G(d) for the C and H atoms of $[\mathbf{2}]^+$; 6-31+G(d) for the C, N, and S atoms of $[\mathbf{1}]^-$.

types of AF-coupled pairs, i.e., $[\mathbf{1}]^-\cdots[\mathbf{1}]^-$ and $[\mathbf{2}]^+\cdots[\mathbf{2}]^+$. This rather simple magnetic structure became evident only because of the comprehensive quantum chemical calculations highlighting their importance for a decent understanding of the magnetic properties of noncommon derivatives (cf. refs 7 and 38).

For the magnetic motif based on AF-coupled $[\mathbf{1}]^-\cdots[\mathbf{1}]^-$ and $[\mathbf{2}]^+\cdots[\mathbf{2}]^+$ pairs, theoretical $\chi(T)$ and $\mu_{eff}(T)$ dependences were calculated with the formulas (5)−(7). Figure 4 demonstrates that the experimental $\chi(T)$ and $\mu_{eff}(T)$ are very well reproduced by this model. The experimental J value for the $[\mathbf{1}]^-\cdots[\mathbf{1}]^-$ pair ($J_1 = -40 \pm 9$ cm^{-1}) is in reasonable agreement with the values calculated using the BS UB3LYP/6-31+G(d) (-61 cm^{-1}) and CASSCF(10,10)/6-31+G(d) (-15.3 cm^{-1}) approaches. The experimental J value for the $[\mathbf{2}]^+\cdots[\mathbf{2}]^+$ pair ($J_2 = -0.58 \pm 0.03$ cm^{-1}) is also in good agreement with the result of the BS calculations (-0.33 cm^{-1} at the UPBE0 level and -0.28 cm^{-1} at the UB3LYP level), whereas the CASSCF technique noticeably underestimates AF interaction in this case (-0.08 cm^{-1}).

Conclusions

Under mild conditions, **2** readily reduced **1** to its RA isolated from the reaction mixture in the form of stable heterospin salt $[\mathbf{2}]^+[\mathbf{1}]^-$ (**3**) ($[\mathbf{2}]^+$, $S = {}^3/_2$; $[\mathbf{1}]^-$, $S = {}^1/_2$). Salt **3** is the first example of a heterospin chalcogen−nitrogen π-heterocyclic RA salt. As compared with the previously studied homospin RA salt $[CoCp_2^*]^+[\mathbf{1}]^-$,[6a] changing the spin state of the cation from $S = 0$ to ${}^3/_2$ does not change the AF character of the exchange interactions in the spin system. As a result, the salt **3** is different from analogous salts $[\mathbf{2}]^+$-$[TCNE]^-$ and $[\mathbf{2}]^+[TCNQ]^-$, having T_C values of 3.7 and 3.1 K, respectively.[11] Comparing the crystal packing of these $[\mathbf{2}]^+$ salts reveals that a change of the anion from $[TCNE]^-$ and $[TCNQ]^-$ to $[\mathbf{1}]^-$ leads to dramatic structural reorganization, in particular to the disappearance of chains of alternating cations (donors, D^+) and anions (acceptors, A^-), $\cdots D^+A^-D^+A^-\cdots$, typical of the former salts.

According to the CASSCF and BS DFT calculations and in agreement with the experiment, the magnetic structure of **3** can be described as a set of AF-coupled $[\mathbf{1}]^-\cdots[\mathbf{1}]^-$ and $[\mathbf{2}]^+\cdots[\mathbf{2}]^+$ pairs only. The exchange interactions in the $[\mathbf{1}]^-\cdots[\mathbf{2}]^+$ pairs are insignificant, which is in strict contrast to the situation in $[\mathbf{2}]^+[TCNE]^-$ and $[\mathbf{2}]^+[TCNQ]^-$ salts.[11]

A way of enforcing anion−cation exchange interactions in the type of salts discussed, together with controlling their sign, might be to use ligand-free transition-metal paramagnetic cations.

Acknowledgment. The authors are grateful to Deutsche Forschungsgemeinschaft (Project 436 RUS 113/967/0-1 R), the Russian Foundation for Basic Research (Project 10-03-00735), the Presidium of the Russian Academy of Sciences (Project 18.17), and the Siberian Branch of the Russian Academy of Sciences (Project 105) for financial support of this work. Support of the work by the Siberian Supercomputer Center and the Ohio Supercomputer Center is also gratefully acknowledged. A.V.L. is grateful to the Russian Academy of Sciences for the Golden Medal with Premium for Graduates 2009 and appreciates the support from the Russian Federal Agency for Education [Grant NK-386P(3) under Contract P2056] and from the Deutscher Akademischer Austausch Dienst−Russian Ministry for Education and Science joint program "Mikhail Lomonosov" (Project 2.2.2.3/9031).

Supporting Information Available: Crystallographic data (120 K) and details of the calculations. This material is available free of charge via the Internet at http://pubs.acs.org.

(38) Gorelik, E. V.; Ovcharenko, V. I.; Baumgarten, M. *Eur. J. Inorg. Chem.* **2008**, 2837–2846.